Effect of cross-linker geometry on dynamic mechanical properties of nematic elastomers

S. M. Clarke,* A. Hotta, A. R. Tajbakhsh, and E. M. Terentjev†
Cavendish Laboratory, University of Cambridge, Madingley Road, Cambridge CB3 0HE, United Kingdom
(Received 30 August 2001; published 18 January 2002)

We study three monodomain (single-crystal) nematic elastomer materials, all side-chain siloxane polymers with the same mesogenic groups but with different types of cross linking: (i) short flexible siloxane linkage affine to the network backbone, (ii) short flexible aliphatic cross links miscible with mesogenic side-chain groups, and (iii) long segments of main-chain nematic polymer. The dynamic mechanical response of these three systems shows a characteristically universal decrease of storage modulus and a corresponding increase of loss factor. This effect of ''dynamic soft elasticity'' is strongly anisotropic, depending on the nematic director orientation. We examine the important role of the average backbone chain anisotropy $r(T)=l_{\parallel}/l_{\perp}$, which is affected by the cross-linking geometry and contributes to the magnitude and frequency dependence of the dynamic anomaly, and discuss possible applications in mechanical damping and polarized acoustic technology.

DOI: 10.1103/PhysRevE.65.021804 PACS number(s): 61.30.−v, 61.41.+e, 46.40.Ff

I. INTRODUCTION

Liquid-crystalline elastomers presently attract much attention due to the behavior arising from a coupling between the spontaneous orientational ordering and the elastic properties of polymer network. Many unusual physical effects have been identified and reviewed in [1–4]. One of the key equilibrium effects is a macroscopic phenomenon of ''soft elasticity'' [5] (see also [6,7]). In conventional elastomers and gels the entropic cost of deforming the average (spherical) backbone polymer coil provides the restoring force and the resulting rubber elasticity. When the network strands are spontaneously anisotropic (ellipsoidal), then instead of deforming the average polymer conformation, some strains could be completely accommodated by simply rotating the average chain distribution without changing its shape. Accordingly, no elastic energy cost would be paid for such deformations. In many cases the ideal soft response cannot be achieved, but one still finds a signature of soft elasticity in the decrease of one of the shear moduli for the same deformation modes that would lead to a complete softness in an ideal nematic network [8].

In contrast to their equilibrium properties, the dynamics of liquid-crystalline elastomers is studied much less. However, important questions arise and so do the expectations of related physical effects. How does the dynamics of internal director rotation, and the corresponding time-dependent softening of the rubber-elastic response, determine the dynamic mechanical response of a nematic rubber? In a study of this kind, Gallani *et al.* [9] studied the stress response to an imposed oscillating shear. Although a polydomain elastomer has been examined, the authors reached a conclusion that the response ''...is insensitive to the isotropic-nematic transition'' and only obtained a nontrivial result in the smectic-*A* phase. Subsequent studies of aligned monodomain elastomers [10] also did not find any unusual effect in the nematic phase and went on to investigate the mechanical effects in the smectic-*A* phase. Some of the reasons that no exceptional effects were found in the nematic phase by [9,10] could be that (i) the nematic region for the materials studied was only $\sim 7°$ and smectic pretransitional effects were important, and (ii) the authors aimed to plot the whole range of dynamic modulus, including very high glassy values at low temperatures, thus masking a subtle nematic region. More recently [11], it has been theoretically demonstrated that a dramatic reduction of storage modulus G' and the associated increase in the loss factor $\tan\delta$ should be expected in monodomain nematic elastomers sheared in certain geometries (cf. Fig. 3 below). This effect has been indeed observed experimentally [12,13]. The analysis of ''dynamic soft elasticity'' allows one to directly probe the basic equilibrium properties of nematic rubbers and also access the new kinetic parameters—viscous coefficients and relaxation times.

In this paper we examine this effect in some detail. We study three types of nematic elastomer materials, having essentially the same chemical structure and composition of side-chain polysiloxane nematic polymer strands but different in the type of cross-linking. We establish the network using exactly the same concentration (by reacting bonds) of difunctional cross-linking groups that are (i) short flexible dimethylsiloxane chains, (ii) hydrocarbon divinyl alkenebenzene units, and (iii) long chains of main-chain nematic polymer which create an additional (and very high) anisotropy in the composite material. In all cases we prepare uniformly aligned monodomain nematic networks—single-crystal liquid-crystal elastomers in the original terminology of Küpfer and Finkelmann [14]. An earlier paper [15] has reported some remarkable differences in equilibrium properties between these three groups of materials, summarized by the great variation of the effective backbone anisotropy of chains making the rubbery network, expressed by a dimensionless ratio of principal step lengths along and perpendicular to the nematic director, $r=l_{\parallel}/l_{\perp}$, and the anisotropy of equilibrium rubber modulus for extensions along and perpendicular to **n**.

Here we aim to establish a similar correlation between the microstructure of the three materials and their dynamic-mechanical response. For an aligned monodomain nematic

*Present address: The BP Institute, University of Cambridge, Cambridge CB3 0EZ, UK.
†Email address: emt1000@cam.ac.uk

rubber we find a strong dependence on the displacement orientation. In the shear geometry where the director is forced to rotate, the characteristic decrease of storage modulus and the increase of loss are observed, while in the neutral ''log-rolling'' geometry the rubber responds as an isotropic elastic medium. This key feature of dynamic soft elasticity is universal, but the magnitude of the effect depends strongly on the internal backbone anisotropy r and varies greatly between the three materials. The most unexpected result is the response frequency dependence. Although the nematic rubbers are known to have very slow relaxation modes, the observed increase in the internal mechanical dissipation is more pronounced at high frequencies. The traditional way to analyze the dynamic mechanical thermal analysis and instruments (DMTA) data is by constructing master curves by time-temperature superposition of measured response and extrapolating the data to either very long times or very high frequencies [16]. In nematic rubbers, where the main effects occur due to the nematic transition, one cannot directly apply such superposition, since the results at higher temperature represent a completely different (isotropic) physical system.

After briefly describing (in Sec. II) the material composition, transition temperatures and the equilibrium anisotropy, in Sec. III we report on the detailed results of dynamic-mechanical measurements. Section IV is the discussion, where we bring the results together and compare with the theory [11]. Finally, in the Conclusion, we speculate about the possible applications of dynamic soft elasticity in two areas of modern technology: the mechanical damping coatings of engineering components and the acoustic polarization devices.

II. EXPERIMENT

Samples of side-chain siloxane liquid-crystalline elastomers were prepared in the Cavendish Laboratory following the procedure of Finkelmann *et al.* [14,17,18], with three different cross linkers. We would like to refer the reader to a preceding paper (on equilibrium properties of the same materials) [15] for the chemical and preparation details, also summarized in Fig. 1 and Table I. One brief explanation of composition choice is due here. Calculating the cross-linking density by reacting bonds, as described above, could be quite different from the actual concentration of the species in a resulting material. In particular, in the case of main chain (MC) polymer cross linker (75 rodlike monomers long), the relative gram weight in the otherwise side-chain polymer matrix is very high. One may equally regard such a system as a main-chain nematic rubber network, end linked with relatively small cross-linking groups made of side-chain nematic polysiloxane. The composition close to the borderline, when the overall mass of MC material in the network is approximately equal to that of side-chain polysiloxane, is achieved for crosslinking by a combination of approximately 1 mol % of MC and 9 mol % of 11UB. Accordingly, there are two MC-containing materials described in this article—the ''optimal'' composition of (1 part MC and 9 parts 11UB), referred to as SiMC in Table I, and the fully-MC cross-linked network, named SiMC10. Few practical results could be obtained on SiMC10 because of its extremely slow response and mechanical recovery, which we assert is due to the restriction of chain mobility by sharp hairpins in the nematic phase of the MC polymer.

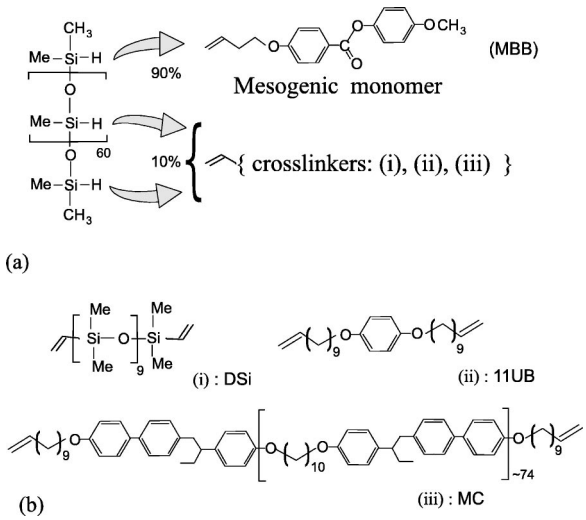

FIG. 1. Schematic illustration of the materials used in this paper. (a) Siloxane backbone chain with Si-H groups reacting with 90 mol % mesogenic phenyl-benzoate side groups, MBB and 10 mol % of divinyl cross-linking groups; (b) flexible siloxane chain, DSi (giving the SiF sample), flexible small-molecule 1,4 alkeneoxybenzene, 11UB (resulting in the SiH material), and the main-chain nematic polymer of 1-biphenyl-2-phenyl butane, MC (giving the two SiMC materials).

Equilibrium transition temperatures given in the Table I were determined on a Perkin Elmer, Pyris 1 differential scanning calorimeter, extrapolating to low cooling rates. The DMTA measurements were performed on a dedicated Metravib RDS Viscoanaliser VA4000 in the shear sandwich geometry. The DMTA device was calibrated prior to measurement. We used thin circularly cut samples, which were approximately 6 mm in diameter and 0.25 mm thick, measured by micrometer individually for each sample. The amplitude of the applied deformation was 10 μm, making the simple shear strain $\varepsilon = 4.0\%$. The materials were studied over a temperature range encompassing the glass and the clearing transitions (typically between -20 and 120 °C). Both heating and cooling scans were performed at the temperature sweep rate of 1 °C/min to allow extensive data collection over a wide range of frequencies (from 0.1 to 100 Hz).

The key output result of a DMTA measurement of viscoelastic materials is the complex modulus G^* depending on frequency and temperature. For an oscillating shear experiment with an imposed strain, say $\varepsilon_{xz} = \varepsilon_0 e^{i\omega t}$, the complex modulus is defined as $G^*(\omega) = \sigma(\omega)/\varepsilon_{xz} = \sigma_0/\varepsilon_0 e^{i\delta}$, where the measured stress $\sigma(\omega) = \sigma_0 e^{i\omega t} e^{i\delta}$ has a phase shift δ, the measure of dissipation in the material. In the following section we present the results for two key characteristics: the real part G' of the complex modulus $G^*(\omega)$ (called the storage modulus, a measure of elastic energy stored in the material) and the loss factor $\tan\delta$, at several selected frequencies, as a function of temperature.

TABLE I. Proportions (in mol %) of cross linkers DSi, 11UB, and MC in the overall cross-linking composition (of the fixed total of 10%), the corresponding volume fraction of the side-chain mesogenic polymer (in wt. %), and temperatures of glass and nematic-isotropic transitions. The glass transition temperatures are approximate, with an error of at least ±5°.

Samples	%(DSi)	%(11UB)	%(MC)	SC content	T_g (°C)	T_{ni} (°C)
SiF	10	0	0	78%	−3	68
SiH	0	10	0	87%	3	86
SiMC	0	9	1	42%	2	107
SiMC10	0	0	10	7%	17	108

The slow heating and cooling rates allowed the linear dynamic response to settle, even when it was changing rapidly with temperature. However, the hard brittle nature of the materials in the glassy phase often resulted in slip in the shear sandwich sample geometry. Therefore, only data some 10 or more degrees above the glass transition T_g are considered reliable. However, since we are principally concerned with liquid-crystalline effects that occur at high temperatures, these issues did not constitute a problem for our paper.

Figure 2 summarizes the equilibrium thermal expansion data. The spontaneous change in length of the sample along the uniform nematic director **n** occurs on changing the temperature and, accordingly, the underlying nematic order $Q(T)$. The measured length $L(T)$ is normalized with respect to the constant sample length L_0 in the isotropic state above the nematic transition temperature T_{ni}, to provide the spontaneous uniaxial deformation $\lambda_{th}=L/L_0$. Clearly, the difference in cross-linker properties has a profound effect on the magnitude of spontaneous deformation. The earlier detailed study [15] has obtained a good linear relationship with the order parameter, $\lambda_{th}=1+\alpha Q$, but with a very different slope: the fitting gives $\alpha=0.08$, 1.02, and 2.8 for the three samples, SiF, SiH, and SiMC, respectively. The theory of equilibrium ideal nematic elastomers [8] calculates this strain as a unique function of the effective mechanical anisotropy of polymer backbones of the network. This anisotropy is directly experimentally measured as, for instance, the ratio of principal radii of gyration $R_\parallel/R_\perp$ (see, e.g., [19]). The theory uses the parameter $r=l_\parallel/l_\perp$, the ratio of principal step lengths of the ideal nematic network strand [equally, $r=(R_\parallel/R_\perp)^2$ for the principal gyration radii] and obtains the spontaneous deformation $\lambda_{th}=r^{1/3}$. In more complex non-ideal elastomers, the relation between the parameter r, calculated from the uniaxial thermal expansion $(L/L_0)^3$, and the principal chain step lengths may be less clearly defined. Nevertheless, the effective anisotropy of network backbone, $r(T)$, has to be a function of nematic order; in the isotropic phase above T_{ni} one recovers $r=1$.

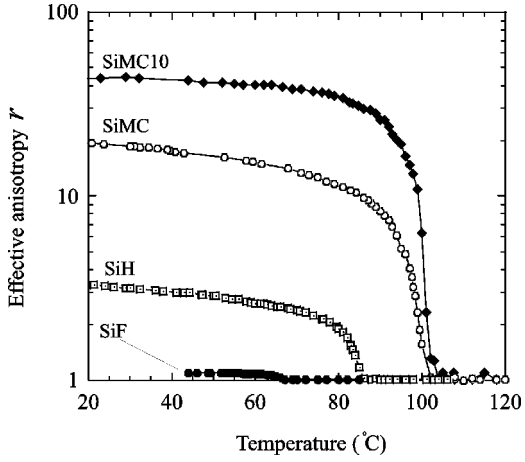

FIG. 2. Thermal expansion data for monodomain polysiloxane nematic elastomers: SiF, SiH, SiMC, and SiMC10 (labeled on the plot). The data presents the effective anisotropy ratio r calculated as a cubic power of spontaneous uniaxial expansion, $r=(L/L_0)^3$, on cooling of freely suspended rubber strips, cf. [15] for detail. The logarithmic scale of the r axis allows all data to be displayed on the same graph.

III. DMTA RESPONSE

In a study of linear dynamic-mechanical response of monodomain nematic rubber, we shall examine the contrasting simple shear geometries, as shown in Fig. 3. A geometry of uniaxial extension, more commonly found in studies of equilibrium stress strain in elastomers, is less appropriate for an oscillating regime because of slow relaxation and incomplete sample recovery on each cycle. The oscillating simple shear $\varepsilon_{xz}(t)$, is externally applied to the sample. In our setup we were able to examine and compare the response in the (D) displacement geometry, where one expects to find the signature of internal director relaxation, and the ''log-rolling'' (V)

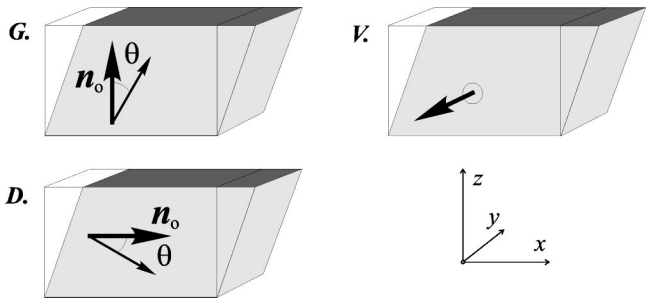

FIG. 3. The geometry of simple shear with three principal orientations of the initial director **n** labeled **G** (for **n** along the shear gradient), **D** (displacement), and **V** (vorticity). The small-amplitude shear ε_{xz} is applied to the elastomer and the measured stress $\sigma_{xz}(\omega)$ provides the linear-response modulus in each of the three configurations.

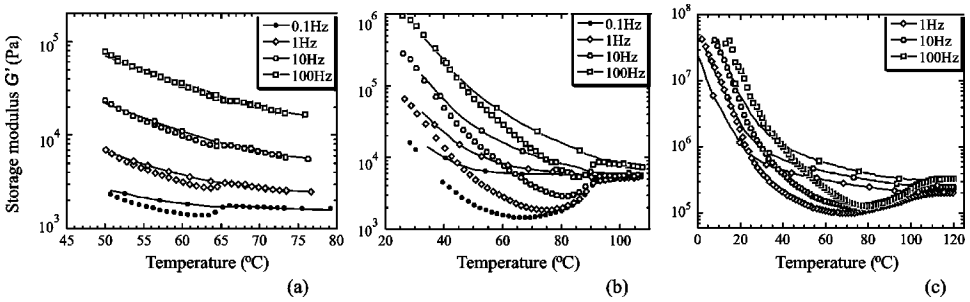

FIG. 4. Linear dynamic-mechanical response of the weakly anisotropic SiF sample, (a) the SiH sample with the medium backbone anisotropy, and (b) the strongly anisotropic SiMC sample, (c) as a function of temperature. Raw values of storage shear modulus G' (logarithmic scale) at frequencies 0.1, 1, 10, and 100 Hz (labeled on plot); data are plotted for two geometries, D (symbols) and V (continuous lines).

vorticity geometry, where the ideally aligned monodomain nematic rubber should not have any induced director rotation.

A. Storage modulus G'

Figure 4 presents the temperature dependence of storage elastic modulus G' at frequencies of 0.1, 1, 10, and 100 Hz for the sample SiF having low-anisotropy (a), SiH with the medium anisotropy (b), and SiMC with the high internal polymer chain anisotropy (c). The storage modulus G' falls with increasing temperature, which is a typical characteristic of ordinary polymeric materials and simply reflects the departure from the glassy state. The modulus in the glassy region, at the lowest temperature, could not be obtained as the value reached the maximum limit of force of the DMTA device (one expects the typical glassy values $G' \sim 1 - 10$ GPa).

At temperatures just below the nematic-isotropic transition ($T_{\rm ni} \sim 68\,^{\circ}$C in SiF, for example) there is a clear evidence of an abrupt drop and in the modulus, which is expected theoretically at low frequencies [11]. These dips in the curves, characteristic of the dynamic soft elasticity, can only be observed in the D-geometry orientation of shear, where the deformation geometry involves the internal director relaxation. The dips are becoming clearer and sharper when the effective anisotropy of the sample is getting higher, i.e., when moving to an SiH sample from the SiF. There is a difference in the behavior of SiMC in that the nematic transition signature is not as abrupt in $G'(T)$ variation; the transition appears more diffuse. This is likely to be caused by this effective anisotropy in SiMC which is an average between the two very different components in the composite; it contains side-chain and main-chain nematic polymers in approximately equal proportion. We shall discuss this point later, in the following section. The same samples sheared in the V geometry show no signs of these anomalies in G' and behave as ordinary isotropic rubbers. The contrast between the response in D and V geometry is quite spectacular. However the modulus in both cases converges to the same value above $T_{\rm ni}$ and approaches the same glass plateau at low temperatures. The response at all frequencies behaves in the similar fashion, with higher frequencies giving the higher modulus (as would be expected) but masking the sharp difference between the two shear geometries.

The high-temperature (isotropic) modulus is $G' \sim 0.002$ MPa, or 2 kPa at 1 Hz for SiF; $G' \sim 0.005$ MPa, or 5 kPa for SiH (several times higher than for SiF) and ~ 0.2 MPa or 200 kPa for SiMC (two orders of magnitude higher than for SiF and SiH). The storage modulus G' is much higher in SiMC. The reason for this enhanced stiffness is thought to be due to main-chain entanglements—especially the hairpins, which restrict the chain mobility in the nematic phase [20,21]. On decreasing the temperature of the SiMC sample one finds a very rapid rise of G' towards its glass plateau value, which we attribute to this pronounced reduction of chain mobility in the nematic phase.

B. Ratio of storage modulus

It is essential to separate the effects of the basic polymer glassy dynamics and the specific nematic anomalies. One way, suggested in [11], is to analyze the scaled nondimensional ratio G'_D/G'_V of the moduli measured for the same sample in two geometries, e.g., D and V in Fig. 4. Figure 5 shows the ratio of storage moduli in these two geometries, for several frequencies. As expected, this ratio approaches unity in the isotropic phase. At the nematic transition one finds a very clear and universal drop in G' with an evident superposition of the critical behavior near $T_{\rm ni}$. It is very interesting to note that the critical behavior in SiMC is much more diffuse—although the relative magnitude of the drop is very high. This is likely to be caused by the composite microstructure and the MC content in this composite material, whose effective anisotropy is an average between the two very different components. Accordingly it is plausible that the storage modulus, especially at high frequencies, is not fully equilibrated and lags behind the would-be equilibrium curve.

C. Loss factor tan δ

Figure 6 presents the temperature variation of the loss factor, $\tan\delta = G''/G'$ (the ratio of imaginary and real parts of G^*. One is impressed by the record-high values of this factor, describing the internal mechanical loss in the material. In most polymeric materials $\tan\delta$ is seldom higher than 0.1 and even the characteristic loss peak at the glass transition is

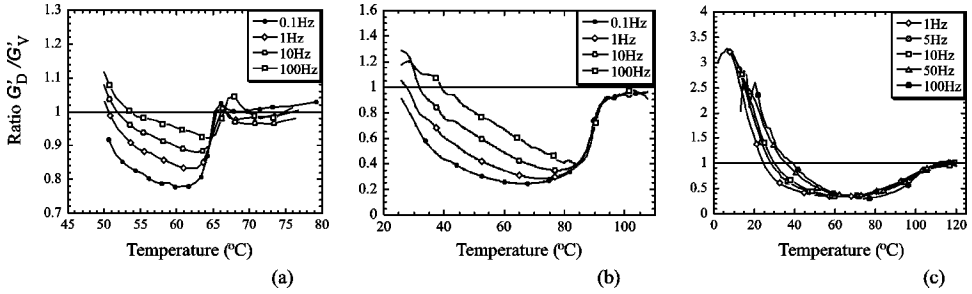

FIG. 5. Scaled nondimensional ratio G'_D/G'_V (linear scale) at frequencies 0.1, 1, 10, and 100 Hz for the SiF (a), SiH (b), and SiMC (c), showing the universal drop at the nematic transition and the frequency dependence predicted by the theory [11]. Note that the linear scale spans from 0 to 1 for SiH and from 0 to 4 in SiMC, in contrast to the SiF sample, where the axis is stretched to highlight the effect.

usually nearly an order of magnitude lower than the values displayed in Fig. 6. One can also notice that the high internal loss is not a particular feature of any phase transformation (as it is the case with the characteristic glassy loss peak in ordinary polymers and rubbers); in the whole region between the T_g and T_{ni} the loss factor is consistently large. This is consistent with the theoretical concept of dynamic soft elasticity [11], which says that the relaxation of internal degree of freedom (the nematic director **n**) causes the softening and high dissipation over the whole nematic range. However, if one follows the theoretical argument to its end, the expectation would be that the loss factor reduces to its common low values in the isotropic phase above T_{ni} (just as the ratio G'_D/G'_V becomes a unity). Instead, we notice that high dissipation persists even above the nematic transition, especially pronounced at high frequencies. Still, there is a clear signature of nematic phase transition, leading to the rapid enhancement of internal mechanical dissipation in the nematic phase.

The qualitative feature of the highest loss factor at high frequencies is again reproduced in SiMC [Fig. 6(c)]. However, there is a clearly nonmonotonic behavior at low frequencies, which has not been observed in either SiF or SiH. Since at high temperatures, above T_{ni}, the loss factor behaves as expected for an isotropic rubber, and the high-frequency tan δ below T_{ni} is the same as for SiF and SiH, we must conclude that the reduced mobility of main-chain strands is due to the reduction of dissipation at low frequencies. At around and above 100 Hz one does not expect that a major backbone rearrangement can occur in the network and the mechanical dissipation should be determined by the vibration of bulky mesogenic side groups (organized along the local nematic director). There are fewer of such side groups in SiMC and thus the overall amount of loss is somewhat lower. Nevertheless, the qualitative features are identical between all three materials. In contrast, at low frequencies the network strands begin responding to the imposed oscillating strain. Here we see a big difference between the flexible-chain SiF and SiH on the one side, and SiMC on the other. In the latter, the main-chain polymers fold into hairpins in the nematic phase and restrict the internal mobility. In fact, this is the reason we do not present the dynamic-mechanical data for the fully main-chain SiMC10; in spite of all efforts we could not obtain any meaningful response at low frequencies at all. It is unfortunate that our experimental DMTA apparatus was unable to test even higher frequencies; in the Conclusion section we shall discuss the possible ways of extrapolating the predictions into the high-frequency region.

IV. CONCLUSION

In this paper we have demonstrated the highly anisotropic behavior of three nematic liquid-crystalline elastomers to small-amplitude oscillatory shear. The type of network cross linker makes a significant difference in the equilibrium properties of these elastomers, in particular, in their effective anisotropy. In contrast, the observed dynamic-mechanical behavior is very similar. Apart from some quantitative differences (most noticeable in the ''bare'' magnitude of the storage modulus G') the main features of composite materi-

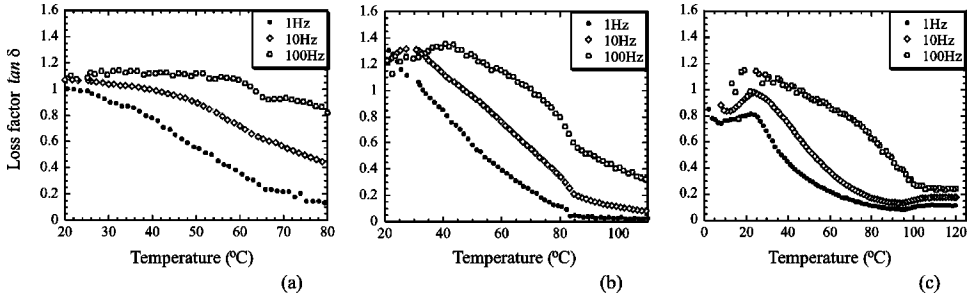

FIG. 6. The loss factor tan $\delta = G''/G'$, for the SiF sample (a), SiH sample (b), and SiMC sample (c) in the *D* geometry, at frequencies 1, 10, and 100 Hz. The high-frequency curve in SiMC is very similar to that of SiH (with a certain overall magnitude reduction). The internal mechanical loss in SiMC is nonmonotonic at loss frequencies, with an unexpected reduction just below T_{ni} (see text).

als SiF, SiH, and SiMC are very similar. The universality of dynamic soft elasticity is best represented by the scaled modulus ratio, which to a large extent eliminates the dependence on the underlying polymer glassy dynamics.

These marked effects are nearly independent of the nature of the polymer backbone. We reiterate that the observed effects are based on the physics of dynamic soft elasticity, due to the internal relaxation of nematic director, and has nothing to do with traditional mechanisms of damping in polymeric systems [16]. At first glance, one is concerned that the real and imaginary parts of the complex modulus G^* do not seem to satisfy the Kramers-Krönig relation, which would demand the rise in G'' (and thus $\tan\delta$) in response to a rapid rise in G'. The fact that we have a consistently high loss over the whole nematic region, where G' behaves nonmonotonically, is most likely the indicator of the fact that the dynamic-mechanical response is not linear. Indeed, even the equilibrium theory predicts a soft-elasticity effect of strain-dependent drop in the modulus in the D geometry where the internal director rotation occurs. We assume the phenomenon is the same in the oscillating dynamic regime and, thus, the standard linear-response arguments should not directly apply to the results.

This paper demonstrates the potential for nematic liquid-crystalline elastomers in mechanical damping applications. These materials have very large loss factors over wide ranges of temperature and frequency. In particular, the highest dissipation was found at higher frequencies ($\geqslant$100 Hz) which is potentially very useful for many acoustic and vibration damping applications. Liquid-crystalline elastomer materials can be prepared with several mesophases in the rubbery temperature region, and hence with a number of phase transitions that could also give rise to critical fluctuations and mechanical loss. However, there are indications that this would not lead to more effective damping. In fact, the presence of smectic phases has an effect of increasing mechanical rigidity and reducing the loss factor in comparison with a purely nematic material [22].

Another attractive physical property, with a high potential in acoustic applications, is the anisotropy of dynamic soft elasticity. As with its equilibrium counterpart, only some selected modes of deformation are affected. This may lead to a whole new technology of manipulating acoustic wave polarization in a similar way to the traditional optical birefringence of liquid crystals. In nematic rubbers, acoustic shear waves would be effectively dissipated when they propagate in the D or G geometry through a monodomain nematic rubber, but would pass through in the V geometry.

ACKNOWLEDGMENTS

The authors thank EPSRC (A.R.T.) and Bridgestone Corporation (A.H.) for funding this work, and Wacker Chemie for the donation of the platinum catalyst. We are indebted to H. Finkelmann for the advice and assistance in chemical preparations. Many discussions with F. Elias, M. Warner, G. R. Tomlinson, and C. Remillat are gratefully appreciated.

[1] W. Gleim and H. Finkelmann, in *Side-Chain Liquid Crystal Polymers*, edited by C. B. McArdle (Blackie and Sons, Glasgow, 1989).
[2] G. G. Barclay and C. K. Ober, Prog. Polym. Sci. **18**, 899 (1993).
[3] H. R. Brand and H. Finkelmann, in *Handbook of Liquid Crystals*, edited by D. Demus *et al.* (Wiley-VCH, Weinheim, 1998).
[4] E. M. Terentjev, J. Phys.: Condens. Matter **11**, R239 (1999).
[5] M. Warner, P. Bladon, and E. M. Terentjev, J. Phys. II **4**, 91 (1994).
[6] L. Golubovic and T. C. Lubensky, Phys. Rev. Lett. **63**, 1082 (1989).
[7] P. D. Olmsted, J. Phys. II **4**, 2215 (1994).
[8] M. Warner and E. M. Terentjev, Prog. Polym. Sci. **21**, 853 (1996).
[9] J. L. Gallani, L. Hilliou, P. Martinoty, F. Doublet, and M. Mauzac, J. Phys. II, **6**, 443 (1996).
[10] J. Weilepp, P. Stein, N. Assfalg, H. Finkelmann, P. Martinoty, and H. R. Brand, Europhys. Lett. **47**, 508 (1999).
[11] E. M. Terentjev and M. Warner, Eur. Phys. J. E **4**, 343 (2001).
[12] S. M. Clarke, A. R. Tajbakhsh, E. M. Terentjev, and M. Warner, Phys. Rev. Lett. **86**, 4044 (2001).
[13] P. Stein, N. Assfalg, H. Finkelmann, and P. Martinoty, Eur. Phys. J. E **4, 255**, 262 (2001).
[14] J. Küpfer and H. Finkelmann, Macromol. Chem. Phys. **195**, 1353 (1994).
[15] S. M. Clarke, A. Hotta, A. R. Tajbakhsh, and E. M. Terentjev, Phys. Rev. E **64**, 061702 (2001).
[16] J. D. Ferry, *Viscoelastic Properties of Polymers* (Wiley, New York, 1980).
[17] H. Finkelmann, A. Greve, and M. Warner, Eur. Phys. J. E **5**, 281 (2001).
[18] H. Wermter and H. Finkelmann, e-Ploymers (www.e-polymers.org), No. 013 281 (2001).
[19] V. Castelletto, L. Noirez, and P. Vigoureux, Europhys. Lett. **52**, 392 (2000).
[20] F. Elias, S. M. Clarke, R. Peck, and E. M. Terentjev, Europhys. Lett. **47**, 442 (1999).
[21] A. R. Tajbakhsh and E. M. Terentjev, Eur. Phys. J. E, **6**, 181 (2001).
[22] S. M. Clarke, A. R. Tajbakhsh, E. M. Terentjev, C. Remillat, G. R. Tomlinson, and J. R. House, J. Appl. Phys. **89**, 6530 (2001).